Bioconjugate Chemistry

Article

pubs.acs.org/bc

New Generation of Bioorthogonally Applicable Fluorogenic Dyes with Visible Excitations and Large Stokes Shifts

András Herner,[†] Gemma Estrada Girona,[‡] Ivana Nikić,[‡] Mihály Kállay,[§] Edward A. Lemke,[‡] and Péter Kele*,[†]

[†]"Lendület" Chemical Biology Research Group, Research Centre for Natural Sciences, Institute of Organic Chemistry, Hungarian Academy of Sciences, Magyar tudósok krt. 2., H-1117 Budapest, Hungary

[‡]Structural and Computational Biology Unit, European Molecular Biology Laboratory, Meyerhofstrasse 1., D-69117 Heidelberg, Germany

[§]MTA-BME "Lendület" Quantum Chemistry Research Group, Department of Physical Chemistry and Materials Science, Budapest University of Technology and Economics, P.O. Box 91, H-1521 Budapest, Hungary

Supporting Information

ABSTRACT: Synthesis of a set of new, azide bearing, biorthogonally applicable fluorogenic dyes with large Stokes shifts is presented herein. To assess the fluorogenic performance of these new dyes we have labeled a genetically modulated, cyclooctyne-bearing protein in lysate medium. Studies showed that the labels produce specific signal with minimal background fluorescence. We also provide theoretical insights into the design of such fluorogenic labels.

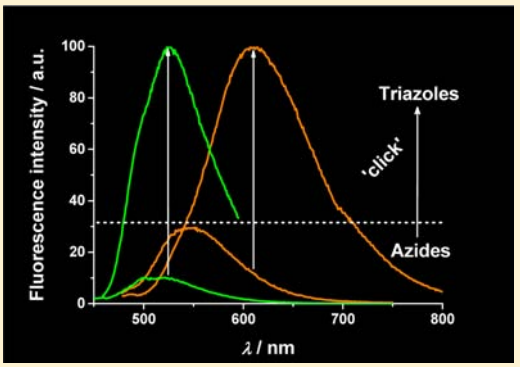

INTRODUCTION

Modulation of biomolecules by fluorescent tags is of great importance in biological research.[1−3] The popularity of fluorescent manipulation of biological matter can be owed to the highly sensitive and relatively cheap detectability of the fluorescent signal with remarkable spatial and temporal resolution, as well as their potential for multichannel imaging.[4] Indeed, labeling of proteins, lipids, nucleic acids, sugars, or even cells and viruses with synthetic fluorescent dyes has become an indispensable tool in bioanalytical sciences.[1−3,5−7] A special class of fluorescent markers is represented by fluorogenic labels.[8−13] The characteristic feature of fluorogenic markers is that their fluorescence intensity increases upon reacting with their target biomolecules. Due to the distinct features of the dark and emissive forms high signal-to-noise ratios are achieved, which is particularly demanded in fluorescent technologies like super resolution imaging techniques.[14]

In fluorescent live cell labeling schemes it is very important that the chemical transformation is biocompatible, fast, and high yielding, so bioorthogonal functions and reactions are the methods of choice.[15−19] Bioorthogonal tagging reactions have benefited greatly from the use of the azide group.[20,21] Several examples demonstrated the advantages of its highly energetic yet quite stable nature in bioorthogonal transformation schemes. Noteworthy is its selective reactivity with (cyclo)-alkynes and phosphanes that enables reactions solely with these particular functions even in the presence of several other functional groups present in biological media.[22−25] Another, less emphasized feature of the azide group is the fact that its incorporation into fluorescent frameworks often results in dramatic drop in fluorescence intensity.[10,26,27] Importantly, the originally quenched fluorescence reinstates upon the conversion of azides into amines or triazoles.[26,27] Quite simply, under suitable circumstances incorporation of azide moiety into fluorescent scaffolds offers a two-in-one combination of bioorthogonality and fluorogenicity. Despite their obviously advantageous features azido quenched fluorescent tags are rarely reported. Design of fluorogenic labels mostly relies on empirical trial and error methods and very few examples use theoretical prediction of such features.[27] Recently we have introduced new azide quenched frameworks whose spectral and fluorogenic features were predicted with good reliability.[28] These probes exhibited excellent fluorogenic properties; however, all showed excitation maxima in the UV region. Therefore, using the same prediction methodology, we intended to design new azide-quenched fluorogenic probes with excitation wavelengths preferably in the visible region and

Received: May 27, 2014
Revised: June 16, 2014
Published: June 16, 2014

   dx.doi.org/10.1021/bc500235p | *Bioconjugate Chem.* 2014, 25, 1370−1374

emission bands in the red regime of the electromagnetic spectrum.

RESULTS AND DISCUSSION

Using empirical methods we have designed frameworks **5**–**6** (Figure 1.). Density functional theory (DFT) calculations were also run to predict characteristic photophysical features, namely, absorption and emission maxima and oscillator strengths of transitions.

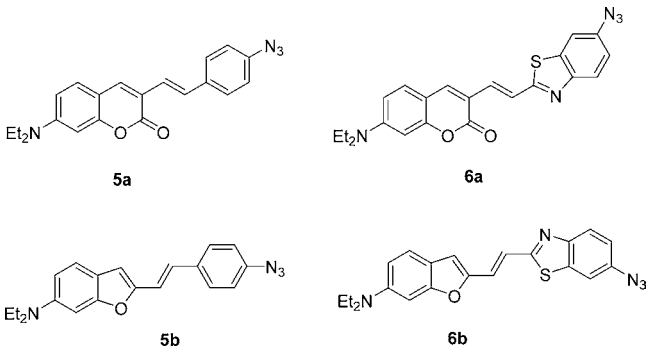

Figure 1. Proposed fluorogenic and bioorthogonally applicable scaffolds.

To obtain **1a** and **1b** (Scheme 1) the corresponding carbaldehydes were condensed with 2-(4-nitrophenyl)acetic acid. In case of **2a** and **2b** the carbaldehydes were allowed to react with 2-methyl-6-nitro-1,3-benzothiazole in molten *p*-toluenesulfonic acid. The nitro derivatives **1** and **2** were reduced with tin(II) chloride in aqueous hydrochloric acid to furnish the corresponding amines, **3** and **4**. It is worth mentioning that in case of **1b** two products were formed in similar ratio under these conditions, e.g., **3b** and its chlorinated congener. In order to avoid chlorination at the 3-position of the benzothiazole ring the reduction step was carried out in absolute ethanol using anhydrous tin(II) chloride. Transformation of the amines to the corresponding azides **5** and **6** was effected by diazotization and subsequent exchange with sodium azide (Scheme 1).

In order to compare the spectral properties of the azides with their triazole congeners compounds **5** and **6** were reacted with *N*-(prop-2-ynyl)pivalamide. The 1,3-dipolar cycloaddition of the azides and the alkyne was effected by catalytic amount of $[Cu(PhP_3)_2]NO_3$ in methylene chloride in the presence of triethylamine[29] (see Supporting Information) to obtain triazoles **7** and **8** in good yields.

We have studied the photophysical properties of click-products **7** and **8** in comparison to their parent azides **5** and **6** in CH_2Cl_2, DMSO, and phosphate buffered medium (Table 1) (see Supporting Information, Figure S1).

In line with our expectations and predictions, all azides showed fluorogenic properties. In terms of fluorogenicity, **5b** performed the best. To our delight all triazoles were found to be excitable in the visible range of the spectrum and possessed remarkable Stokes shifts. Fluorogenic compounds with such large Stokes shifts are rarely reported; in fact, to the best of our knowledge the only one with similar properties was reported in our recent work.[28] For each azide–triazole pair we have observed red-shifted emission spectra of the triazoles compared to their corresponding azides. This is most likely in connection with the change in molecular dipole moments associated with the evolution of the triazole motif (Table 1). It should be mentioned that in all cases hydrogen bond formation with water decreased the fluorescence intensities.

Next, we were curious to investigate the performance of our new dyes in a more challenging biological environment. We used Amber suppression to genetically encode an unnatural amino acid (UAA) with a reactive cyclooctyne (bicyclo[6.1.0]-non-4-yn, BCN) site-specifically into nonfluorescent maltose binding protein (MBP).[23,30−32] MBP encoding nonreactive BOC-lysine serves as a negative control to the BCN lysine UAA.

Experiments with MBP were performed for dyes **5a** and **6a** only, since initial experiments with free BCN-Lys justified further elaboration of these two dyes (see Supporting Information, Figure S2). First, purified MBP derivatives (BCN and BOC) were treated with **5a** and **6a** in buffer.

Scheme 1. Synthetic Route to Fluorogenic Labels 5 and 6[a]

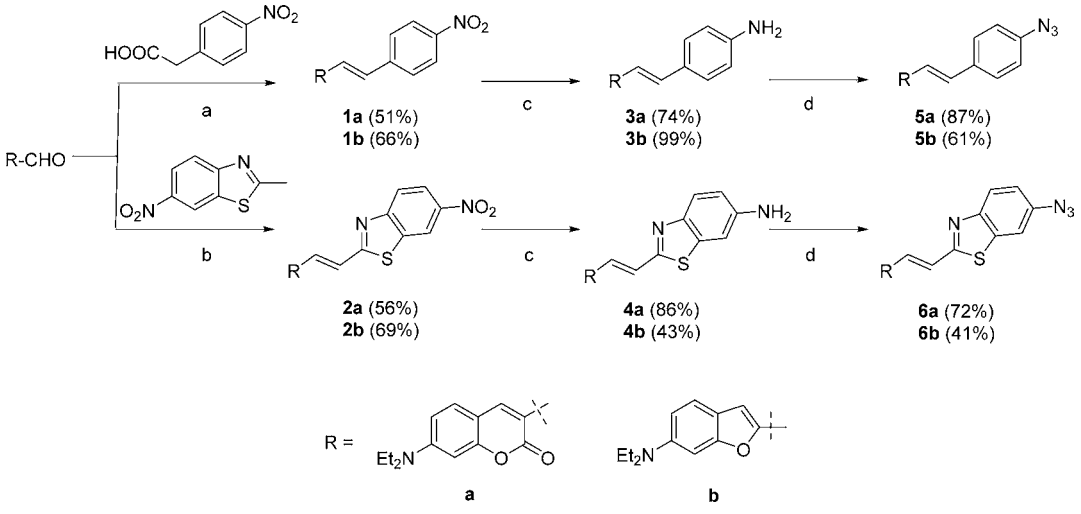

[a](a) Piperidine, 140 °C, 2 h; (b) TsOH × H_2O, 105 °C, 18 h; (c) $SnCl_2$, 40–80 °C, 3 h to 3 d; (d) $NaNO_2$, HCl(aq.), 0 °C, 10 min, then NaN_3 0 °C → r.t., 18 h.

dx.doi.org/10.1021/bc500235p | *Bioconjugate Chem.* 2014, 25, 1370−1374

Table 1. Photophysical Properties of Azides and Triazoles

fluorophore	5a	7a	5b	7b	6a	8a	6b	8b
λ_{max} (abs)/nm[a]	448	433	404	414	478	457	464	468
λ_{max} (abs)/nm[b]	453	441	410	417	478	471	463	469
λ_{max} (abs)/nm[c]	386	394	403	399	436	446	411	452
λ_{max} (exc)/nm[c]	n.a.	442	n.a.	433	n.a.	448	n.a.	445
$\varepsilon/10^4$ $M^{-1}cm^{-1}$[b]	n.a.	4.4	n.a.	3.3	n.a.	4.2	n.a.	3.6
$\varepsilon/10^4$ $M^{-1}cm^{-1}$[c]	n.a.	2.0	n.a.	1.8	n.a.	2.2	n.a.	2.2
λ_{max} (em)/nm[a]	501	505	476	519	512	520	565	576
λ_{max} (em)/nm[b]	510	510	504	545	531	546	599	612
λ_{max} (em)/nm[c]	501	527	503	510	544	607	n.d.[d]	630
Stokes shift/nm[c]	n.a.	133	n.a.	111	n.a.	161	n.a.	178
Φ_F(triaz.)/Φ_F (azide)[b,e]	8.9		62.7		5.0		5.3	
Φ_F (triaz.)/Φ_F (azide)[c,e]	4.4		17.4		4.2		6.0	
I_F(triaz.)/I_F (azide)[b,f]	16.6		121.1		7.4		7.8	
I_F (triaz.)/I_F (azide)[c,f]	12.4		26.3		7.9		9.0	

[a]In CH_2Cl_2. [b]In DMSO. [c]In PBS. [d]Not detectable, in the background. [e]Compared at same absorbances at maxima. [f]Excited and measured at the maxima of the triazoles.

Monitoring of the fluorescence intensities at corresponding wavelengths over 24 h indicated continuously increasing fluorescence in case of MBP-BCN while moderate changes were observed for MBP-BOC (Figure 2A and SI Figure S3).

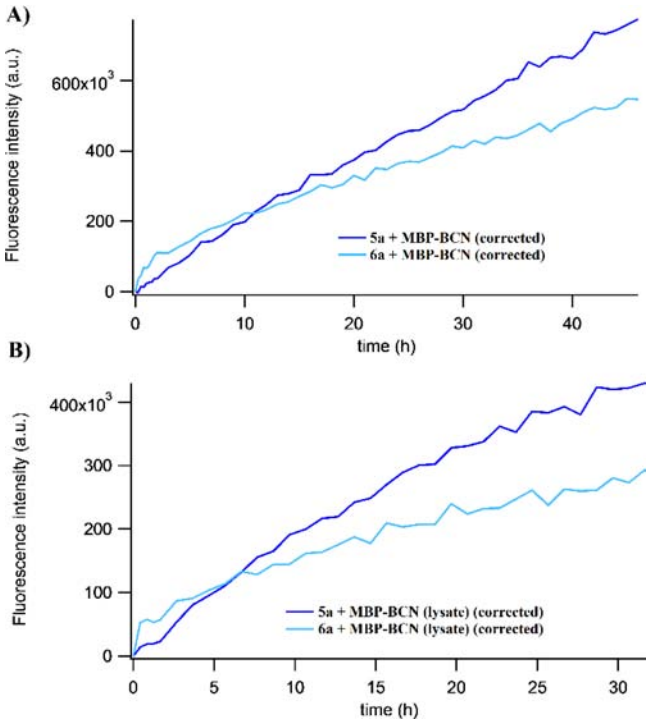

Figure 2. Background corrected fluorescent changes at characteristic emission wavelengths of dyes **5a** and **6a** upon reaction with MBP derivatives in (A) buffered medium (B) in lysate.

The fluorescence intensity recorded for the MBP-BOC system was used as background for correction. Next we repeated these experiments in the presence of *E. coli* lysate. Monitoring of fluorescent changes over time showed similar trends to that observed in pure buffer with just slightly increased background signals (Figure 2B and SI Figure S4). Samples of these experiments were also analyzed on SDS-PAGE. The gels were scanned with a 473 nm laser for fluorescence, then stained with Coomassie Blue (Figure 3).

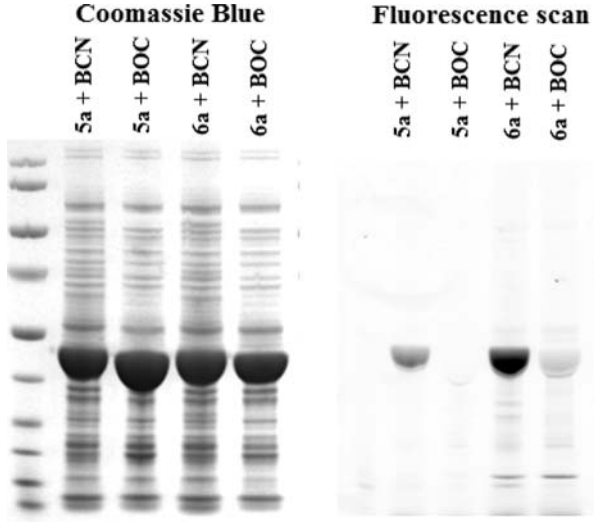

Figure 3. (Left) Coomassie stained and (Right) fluorescent (λ_{exc} = 473 nm) images of reaction products of **5a** and **6a** with MBP derivatives in lysates.

Analysis of the gel under visible light excitation also supported that fluorogenic tags **5a** and **6a** efficiently labeled the BCN tagged MBP. MBP-BOC on the other hand showed very weak or no appreciable fluorescence signal (Figure 3).

It should be noted that due to concentration limit of fluorescence and the speed of the reaction, the experiments were not conducted until reaching a plateau. The results rather reflect qualitative trends as due to the relatively high concentrations of the dyes (50 μM) nonlinear effects, like self-quenching, the fluorescence of the dyes might even appear lower.

From the fluorescent changes (Figure 2) and gel electrophoretic images (Figure 3) we can conclude that the two labels can stand the challenging conditions of lysate medium and only low fluorescent decomposition products are formed. These results suggest that these fluorogenic labels can be used in bioorthogonal fluorescent tagging schemes with low background fluorescence in complex biological environments.

Our continuous aim is to understand the fluorogenic nature of azide quenched fluorescent frameworks. In order to get a better insight into the design of such fluorogenic labels we

dx.doi.org/10.1021/bc500235p | Bioconjugate Chem. 2014, 25, 1370−1374

performed quantum chemical calculations. The detailed description of the computational procedure employed can be found in our previous publication;[28] only a brief summary is given here. All calculations were carried out at the density functional theory (DFT) level using the PBE0 functional[33,34] as well as the 6-311++G** basis set. The solvent effects were taken into account with the aid of the polarized continuum model[35] with dichloromethane as solvent. For the excited states the time-dependent DFT approach[36] was invoked. In our study we employed simplified model systems. For each fluorophore the ethyl groups were replaced by methyl groups, and instead of the click reagent used in the experiments propyne was considered. All calculations were performed using the Gaussian 09 package.[37]

The conclusions which can be drawn from the results of the theoretical calculations are similar to those of our previous paper.[28] The optimized ground-state geometries are planar for the azides, while the triazole ring forms an angle of about 30° with the plane of the phenyl/benzothiazole ring in the case of the triazoles. If the geometry optimization is started from the ground-state-optimized structure, the relaxation of the geometry in the S_1 state is moderate, only the torsional angle formed by the triazole moiety and the phenyl/benzothiazole ring changes considerably, which is between 0° and 20° for the various compounds at the minimum of their S_1 surface. The computed transition wavelengths and oscillator strengths are displayed in Table 2, and we can conclude that the agreement of the experimental and theoretical absorption and emission wavelengths is reasonable.

Table 2. Calculated Transition Wavelengths (λ) and Oscillator Strengths for the Fluorophores[a,b]

	absorption		emission	
compound	λ/nm	osc. strength	λ/nm	osc. strength
		Azides		
5a	447 (448)	1.96	499 (501)	2.01
6a	471 (478)	2.13	519 (512)	2.24
5b	455 (404)	1.60	513 (476)	1.73
6b	506 (464)	1.76	581 (565)	2.01
		Triazoles		
7a	443 (433)	1.93	483 (505)	2.01
8a	468 (457)	2.12	506 (520)	2.26
7b	460 (414)	1.56	491 (519)	1.65
8b	510 (468)	1.72	575 (576)	1.96

[a]Calculated for CH_2Cl_2 by using the polarized continuum model. [b]Numbers in parentheses show the experimental results in CH_2Cl_2.

Obviously, the calculated transition probabilities do not explain the significant difference between the fluorescence intensities of the azides and triazoles. In our previous work[28] we pointed out that the low fluorescence intensities measured for the azide derivatives can be explained by the existence of a radiationless decay channel. The azide group can freely rotate at room temperature, and due to the conformational change the first excited state interchanges with a dark state with a low-lying minimum, which suggests that the system can simply return to its ground state via internal conversion processes. To verify the existence of the nonemissive state for the current compounds the excited-state geometry optimizations were repeated for the azides starting from distorted geometries derived by rotating the azide group around the bond connecting the latter to the phenyl/benzothiazole ring. We successfully found these low-lying states with very low excited state → ground state transition probability, which supports that the fluorescence of the azides considered in this study is also quenched due to a radiationless deactivation process.

We can conclude that our new, bioorthogonally applicable azide quenched fluorogenic labels were found to be efficient in bioorthogonal fluorescent labeling experiments. The visible excitations and the remarkably large Stokes shifts of the labels make these dyes especially applicable, e.g., in energy transfer applications where separation of excitation and emission bands is crucial. We have also provided theoretical insights into the nature of such azide-quenched systems. According to our findings in all cases a nonemissive "dark"-state interchanges with the first excited state. Quenching efficiency of fluorescence of the azides is dependent on the equilibrium of this process. These results can be used in the design process of further fluorogenic dyes with better stability, brightness, and polarity suitable for in vivo imaging.

■ ASSOCIATED CONTENT

Supporting Information

Details of synthetic procedures, characterization data for small molecules, and fluorescence spectra for **5**−**8** are available. Details of protein labeling experiments with further spectra and coordinates for optimized geometries are provided. This material is available free of charge via the Internet at http://pubs.acs.org.

■ AUTHOR INFORMATION

Corresponding Author

*E-mail: kele.peter@ttk.mta.hu.

Notes

The authors declare no competing financial interest.

■ ACKNOWLEDGMENTS

The present work was supported by the Hungarian Scientific Research Fund (OTKA, grant numbers K-100134, K108752 and NN-110214) and the "Lendület" Program of the Hungarian Academy of Sciences (LP2013-55/2013 and LP2013-64/2013). I. N. acknowledges support by an EMBO Long-Term and Marie Curie Fellowship and E. A. L. funding of the DFG Emmy Noether and SPP1623 program.

■ REFERENCES

(1) Sahoo, H. (2012) Fluorescent labeling techniques in biomolecules: a flashback. *RSC Adv. 2*, 7017−7029.

(2) Gonçalves, M. S. T. (2009) Fluorescent labeling of biomolecules with organic probes. *Chem. Rev. 109*, 190−212.

(3) Kele, P., Li, X., Link, M., Nagy, K., Herner, A., Lőrincz, K., Béni, Sz., and Wolfbeis, O. S. (2009) Clickable fluorophores for biological labeling—with or without copper. *Org. Biomol. Chem. 7*, 3486−3490.

(4) Fernández-Suárez, M., and Ting, A. Y. (2008) Fluorescent probes for super-resolution imaging in living cells. *Nat. Rev. Mol. Cell. Biol. 9*, 929−943.

(5) Lee, J. H., So, J.-H., Jeon, J. H., Choi, E. B., Lee, Y.-R., Chang, Y.-T., Kim, C.-H., Bae, M. A., and Ahn, J. H. (2011) Synthesis of a new fluorescent small molecule probe and its use for *in vivo* lipid imaging. *Chem. Commun. 47*, 7500−7502.

(6) Ehrenschwender, T., Varga, B. R., Kele, P., and Wagenknecht, H.-A. (2010) New far-red and near-infrared fluorescent probes with large stokes shifts for dual covalent labeling of DNA. *Chem.—Asian J. 5*, 1761−1764.

(7) Sato, M., Ito, Y., Arima, N., Baba, M., Sobel, M., Wakao, M., and Suda, Y. (2009) High-sensitivity analysis of naturally occurring sugar

chains, using a novel fluorescent linker molecule. *J. Biochem. 146*, 33−41.
(8) Nadler, A., and Schultz, C. (2013) The power of fluorogenic probes. *Angew. Chem., Int. Ed. 52*, 2408−2410.
(9) Nikolova, K., Kaloyanova, S., Mihaylova, N., Stoitsova, S., Chausheva, S., Vasilev, A., Lesev, N., Dimitrova, P., Deligeorgiev, T., and Tchorbanov, A. (2013) New fluorogenic dyes for analysis of cellular processes by flow cytometry and confocal microscopy. *J. Photochem. Photobiol., B: Biol. 129*, 125−134.
(10) Le Droumaguet, C., Wang, C., and Wang, Q. (2010) Fluorogenic click reaction. *Chem. Soc. Rev. 39*, 1233−1239.
(11) Jewett, J. C., and Bertozzi, C. R. (2011) Synthesis of a fluorogenic cyclooctyne activated by Cu-free click chemistry. *Org. Lett. 13*, 5937−5939.
(12) Lukinavičius, G., and Johnsson, K. (2011) Switchable fluorophores for protein labeling in living cells. *Curr. Opin. Biol. 15*, 768−774.
(13) Rong, L., Liu, L.-H., Chen, S., Cheng, H., Chen, C.-S., Li, Z.-Y., Qin, S.-Y., and Zhang, X.-Z. (2014) A coumarin derivative as a fluorogenic glycoproteomic probe for biological imaging. *Chem. Commun. 50*, 667−669.
(14) Maglione, M., and Sigrist, S. J. (2013) Seeing the forest tree by tree: super-resolution light microscopy meets the neurosciences. *Nat. Neurosci. 16*, 790−797.
(15) Debets, M. F., van Hest, J. C. M., and Rutjes, F. P. J. T. (2013) Bioorthogonal labelling of biomolecules: new functional handles and ligation methods. *Org. Biomol. Chem. 11*, 6439−6455.
(16) Karver, M. R., Weissleder, R., and Hilderbrand, S. A. (2012) Bioorthogonal reaction pairs enable simultaneous, selective, multi-target imaging. *Angew. Chem., Int. Ed. 51*, 920−922.
(17) Carroll, L., Evans, H. L., Aboagye, E. O., and Spivey, A. C. (2013) Bioorthogonal chemistry for pre-targeted molecular imaging − progress and prospects. *Org. Biomol. Chem. 11*, 5772−5781.
(18) Patterson, D. M., Nazarova, L. A., and Prescher, J. A. (2014) Finding the right (bioorthogonal) chemistry. *ACS Chem. Biol. 9*, 592−605.
(19) Ramil, C. P., and Lin, Q. (2013) Bioorthogonal chemistry: strategies and recent developments. *Chem. Commun. 49*, 11007−11022.
(20) Debets, M. F., van der Doelen, C. W. J., Rutjes, F. P. J. T., and van Delft, F. L. (2010) Azide: a unique dipole for metal-free bioorthogonal ligations. *ChemBioChem 11*, 1168−1184.
(21) Baskin, J. M., and Bertozzi, C. R. (2010) Copper-free click chemistry: bioorthogonal reagents for tagging azides. *Aldrichimica Acta 43*, 15−23.
(22) Varga, B. R., Kállay, M., Hegyi, K., Béni, Sz., and Kele, P. (2012) A non-fluorinated monobenzocyclooctyne for rapid copper-free click reactions. *Chem.—Eur. J. 18*, 822−828.
(23) Dommerholt, J., Schmidt, S., Temming, R., Hendriks, L. J. A., Rutjes, F. P. J. T., van Hest, J. C. M., Lefber, D. J., Friedl, P., and van Delft, F. L. (2010) Readily accessible bicyclononynes for bioorthogonal labeling and three-dimensional imaging of living cells. *Angew. Chem., Int. Ed. 49*, 9422−9425.
(24) van Berkel, S. S., van Eldijk, M. B., and van Hest, J. C. M. (2011) Staudinger ligation as a method for bioconjugation. *Angew. Chem., Int. Ed. 50*, 8806−8827.
(25) Schilling, C. I., Jung, N., Biskup, M., Schepers, U., and Bräse, S. (2011) Bioconjugation *via* azide−Staudinger ligation: an overview. *Chem. Soc. Rev. 40*, 4840−4871.
(26) Sivakumar, K., Xie, F., Cash, B. M., Long, S., Barnhill, H. N., and Wang, Q. (2004) A fluorogenic 1,3-dipolar cycloaddition reaction of 3-azidocoumarins and acetylenes. *Org. Lett. 6*, 4603−4606.
(27) Shieh, P., Hangauer, M. J., and Bertozzi, C. R. (2012) Fluorogenic azidofluoresceins for biological imaging. *J. Am. Chem. Soc. 134*, 17428−17431.
(28) Herner, A., Nikić, I., Kállay, M., Lemke, E. A., and Kele, P. (2013) A new family of bioorthogonally applicable fluorogenic labels. *Org. Biomol. Chem. 11*, 3297−3306.
(29) Gonda, Zs., and Novák, Z. (2010) Highly active copper-catalysts for azide-alkyne cycloaddition. *Dalton Trans. 39*, 726−729.
(30) Plass, T., Milles, S., Koehler, C., Schultz, C., and Lemke, E. A. (2011) Genetically encoded copper-free click chemistry. *Angew. Chem., Int. Ed. 50*, 3878−3881.
(31) Plass, T., Milles, S., Koehler, C., Szymański, J., Mueller, R., Wießler, M., Schultz, C., and Lemke, E. A. (2012) Amino acids for Diels−Alder reactions in living cells. *Angew. Chem., Int. Ed. 51*, 4166−4170.
(32) Borrmann, A., Milles, S., Plass, T., Dommerholt, J., Verkade, J. M. M., Wießler, M., Schultz, C., van Hest, J. C. M., van Delft, F. L., and Lemke, E. A. (2012) Genetic encoding of a bicyclo[6.1.0]nonyne-charged amino acid enables fast cellular protein imaging by metal-free ligation. *ChemBioChem 13*, 2094−2099.
(33) Perdew, J. P., Burke, K., and Ernzerhof, M. (1996) Generalized gradient approximation made simple. *Phys. Rev. Lett. 77*, 3865−3868. Errata (1997), *Phys. Rev. Lett. 78*, 1396−1396.
(34) Adamo, C., and Barone, V. (1999) Toward reliable density functional methods without adjustable parameters: the PBE0 model. *J. Chem. Phys. 110*, 6158−6170.
(35) Miertuš, S. (1981) Electrostatic interaction of a solute with a continuum. A direct utilization of ab initio molecular potentials for the prevision of solvent effects. *Chem. Phys. 55*, 117−129.
(36) Stratmann, R. E., Scuseria, G. E., and Frisch, M. J. (1998) An efficient implementation of time-dependent density-functional theory for the calculation of excitation energies of large molecules. *J. Chem. Phys. 109*, 8218−8224.
(37) Frisch, M. J., Trucks, G. W., Schlegel, H. B., et al. (2009) *Gaussian 09*, revision B.01, Gaussian, Inc., Wallingford, CT.